CROSS-BISPECTRAL ANALYSIS OF A VIBRATING CYLINDER AND ITS WAKE IN LOW REYNOLDS NUMBER FLOW

STEVE ELGAR
Electrical and Computer Engineering, Washington State University
Pullman, Washington 99164, U.S.A.

AND

C. W. VAN ATTA AND M. GHARIB
Department of Applied Mechanics and Engineering Sciences, University of California
La Jolla, California 92093, U.S.A.

Reprinted from

Journal of Fluids and Structures (1990) **4**, 59–71

Journal of Fluids and Structures (1990) **4**, 59–71

CROSS-BISPECTRAL ANALYSIS OF A VIBRATING CYLINDER AND ITS WAKE IN LOW REYNOLDS NUMBER FLOW

STEVE ELGAR
Electrical and Computer Engineering, Washington State University
Pullman, Washington 99164, U.S.A.

AND

C. W. VAN ATTA AND M. GHARIB
Department of Applied Mechanics and Engineering Sciences, University of California
La Jolla, California 92093, U.S.A.

(Received 18 May 1988 and in revised form 8 June 1989)

Cross-bispectral analysis is used to investigate the coupling between a slender vibrating cylinder and the velocity field in its wake at low Reynolds numbers [$\mathrm{Re} = O(10^2)$]. The velocity field was characterized by a complicated power spectrum, with low frequency peaks as well as upper and lower side band peaks near the primary Strouhal frequency peak and its harmonics. Power spectral and cross-bispectral analyses indicate that the rich structure of the wake velocity power spectra is a direct consequence of the vibrating cylinder. The data suggest the cylinder is coupled to its wake in the sense that the cylinder vibrations introduce motions into the wake at the vibration frequency, and these motions interact nonlinearly within the wake to produce fluctuations at other frequencies. Cross-bispectral analysis isolates the interactions between cylinder vibrations and wake fluctuations.

1. INTRODUCTION

THE ROWS OF VORTICES in the wake of a cylinder have been studied extensively since the early investigations of Strouhal (1878) and Lord Rayleigh (1879). The vortices are alternately shed from the upper and lower surfaces of the cylinder at the Strouhal frequency, which is a function of Reynolds number (Roshko, 1954). Berger & Wille (1972) provide a review of pertinent studies, most of which are primarily concerned with the flow field downstream of the cylinder. Other investigators have studied the effects of a vibrating cylinder on the structure of the vortex streets (for reviews see Berger & Wille, 1972; Koopman, 1967; Griffin & Ramberg, 1974; Bearman, 1984). Cylinder vibrations can effect the three-dimensional structure of the wake (Koopman, 1967; Bloor, 1964; Gerrard, 1966), as described by spanwise correlations, and can result in the production of the well known aeolian tones. When the cylinder is allowed to vibrate, the shedding frequency may differ from the Strouhal frequency for a fixed cylinder owing to tuning between the cylinder and the vortex shedding (Koopman, 1967; Griffin & Ramberg, 1974; Gongwer, 1952; Powell & Shulman, 1962; Griffin, 1978). The velocity fluctuations in the wake of an inflexible rod oscillating at the Strouhal frequency can be reduced relative to the fluctuations downstream of a stationary cylinder in low Reynolds number [$\mathrm{Re} = O(10^2)$] flows (Wehrmann, 1965; Berger, 1967). On the other hand, oscillating cylinders in high Reynolds number

0889–9746/90/010059 + 13 $03.00

[$Re = O(10^5)$] flows have been shown to produce wakes with stronger velocity fluctuations than are found behind fixed cylinders (Toebes, 1969). These studies indicate that the effect of the oscillating cylinder on the strength of wake velocities depends on the phase between cylinder vibrations and vortex shedding.

Most of the investigations cited above primarily use time domain analysis to study the vortices in the cylinder wake. Flow visualization techniques have been used to display characteristics of the wake velocities, while further information is provided by the time series of wake velocities. For example, time series graphs in the high Reynolds number experiments of Toebes (1969) suggest a low frequency modulation (equal to the difference between the Strouhal frequency and the cylinder vibration frequency) in velocity measurements downstream of a vibrating cylinder. Additional information about the wake vortices may be obtained with the aid of frequency domain analysis. For example, recent experiments (Sreenivasan, 1985; Van Atta & Gharib, 1987) in low Reynolds number flows ($40 < Re < 150$) have shown that the power spectra of velocity in the wake of a cylinder can have a rich and complicated structure. By comparing power spectra of velocities measured in the wakes behind vibrating and damped cylinders, Van Atta & Gharib (1987) conclude that many features of the velocity power spectra are related to cylinder vibrations.

The present study uses cross bispectral analysis (defined in Section 3) to investigate the coupling between a vibrating cylinder and the velocity fluctuations in its wake at low Reynolds numbers ($40 < Re < 100$). The cross bicoherence between lateral cylinder oscillations and motions within the wake velocity field isolates the phase coupling between the Fourier modes of the cylinder and the wake. This allows the coupling between cylinder and wake to be studied using the methods of time series analysis, rather than the somewhat heuristic approach of physically damping the cylinder vibrations used by Van Atta & Gharib (1987).

Simultaneous measurements of longitudinal wake velocities and cylinder lateral displacement were made in a low speed wind tunnel (described in Section 2). A variety of velocity flow regimes were investigated, characterized by either narrow, broad or multiple-peaked power spectra (Section 4). During some experimental runs, the wake velocity power spectrum evolved in time. The side bands of an initially narrow power spectral peak increased in level, and additional sharp peaks appeared in the spectrum at frequencies lower than the primary peak frequency. These narrow peaks broadened, and eventually coalesced. The primary peak upper side band also increased in level, and eventually became the dominant spectral peak. This spectral evolution was then reversed, with sharp peaks rising out of the broadened spectrum, and an eventual return to a fairly narrow band power spectrum. These dramatic changes in the wake velocity field occurred simultaneously with changes in the dominant modes of vibration of the cylinder. The evolving coupling between cylinder and wake during these experimental runs cannot be studied by physically altering the cylinder vibrations as was done by Van Atta & Gharib (1987). On the other hand, cross bispectra between the vibrating cylinder and the wake velocity field indicate that the evolving wake is responding to changes in the regime of cylinder vibrations.

2. EXPERIMENTAL ARRANGEMENT

The experiments were carried out in the low speed, low turbulence (u'/U less than 0·05% at a speed of 10 m/s) wind tunnel in the Department of Applied Mechanics and Engineering Sciences at the University of California, San Diego. A detailed description of the experimental arrangement is given in Van Atta & Gharib (1987), while a brief

description is presented here for completeness. The test section was 76 cm × 76 cm × 10 m long. The vortex shedding cylinders were steel music wires mounted horizontally in the tunnel midplane 42 cm downstream of the end of the contraction. They passed freely through clearance holes in the tunnel walls and were supported at their ends outside the tunnel walls. One end was connected to a guitar string machine head used to adjust the tension in the wire. The other end was connected to a small cantilever beam with an attached strain gauge used to measure the tension. For the data reported here, wires of diameter $d = 0{\cdot}0356$ cm and $d = 0{\cdot}0254$ cm were used (Table 1), and the working length of the wire between the two auxiliary supports inside the tunnel was 48 cm. Values for other experimental parameters for each of the data sets investigated are presented in Table 1.

Transverse motions (vibrations) of the cylinder were detected with a GE H13A1 infrared photon coupled interrupter module mounted on a vertical airfoil-shaped strut 15·2 cm from one of the tunnel walls. The photo detector contains a gallium arsenide solid state lamp optically coupled across a 3 mm gap with a silicon photo-transistor. The airfoil-shaped mount was vertically adjustable to maximize the detector output when the cylinder vibrated laterally in the gap. The frequency response of the photo detector was flat from 2 to 10 kHz, and the smallest detectable cylinder displacement was on the order of 10 μ.

A constant temperature hot wire anemometer (DISA 55M01, 1 mm long, 1·5 μ diameter) was used to measure the longitudinal velocity fluctuations in the cylinder wake. The hot-wire probe body entered the wake from below at an angle of 30°, and the hot wire was placed at the mid point of the cylinder length, and positioned near the center of the lower row of wake vortices at a downstream location of about 5 cylinder diameters. For small amplitude fluctuations, it can be shown using King's law that $u'/U \approx 4e'/e$, where e is the (large) mean voltage of the hot-wire signal and e' is the (small) fluctuating voltage. Thus, the power spectra of fluid velocity and voltage are similar, and the normalized bicoherences are identical. The photo-detector calibration curve also was locally linear. Consequently, no calibrations were applied to the hot-wire and photo-detector signals. Accounting for small nonlinearities in the calibration curves would not noticeably effect the cross bicoherences presented here. Moreover, nonlinearities in the instrumentation used to measure cylinder vibrations and wake velocities are independent of each other, and thus do not lead to artificially high cross bicoherence values. The hot-wire probe and a small Pitot-static tube used in conjunction with a Baratron pressure gauge to measure the mean free stream velocity were both mounted on a horizontal airfoil-shaped strut attached to a probe traverse outside the tunnel.

3. BISPECTRAL DEFINITIONS

For a discretely sampled time series $\eta(t)$ with the Fourier representation

$$\eta(t) = \sum_n \{A(\omega_n)e^{i\omega_n t} + A^*(\omega_n)e^{-i\omega_n t}\}, \tag{1}$$

the power spectrum and the cross bispectrum between separate signals $\eta_1(t)$ and $\eta_2(t)$ are defined, respectively, as

$$P(\omega_j) = E[A(\omega_j)A^*(\omega_j)], \tag{2}$$

$$XB(\omega_j, \omega_k) = E[A_1(\omega_j)A_1(\omega_k)A_2^*(\omega_j + \omega_k)], \tag{3}$$

TABLE 1

Values for various experimental parameters for the data sets. The column labeled "Degrees-of-freedom" indicates the number of degrees of freedom in the power-spectral and cross-bispectral calculations of each respective data set.

Data set	Length of sample (s)	Degrees-of-freedom	Wire tension (N)	Free stream velocity (m/s)	Reynolds Number (Re)	Natural frequency of cylinder (Hz)	Cylinder diameter (cm)
1	17·1	1000	4·60	2·40	52·0	234	0·0356
2	17·1	1000	7·70	4·01	65·0	75	0·0254
3	8·5	500	5·16	4·04	87·2	260	0·0356
4	1·7	100	5·16	4·04	87·2	260	0·0356

where ω is the radian frequency, the subscripts j, k are frequency (modal) indices, the A_1 are the complex Fourier coefficients of one signal (e.g. wake velocity) and the A_2 are simultaneously measured Fourier coefficients of the other signal (e.g. cylinder displacement), an asterisk indicates complex conjugate, and $E[\,]$ is the expected-value, or average, operator. The normalized magnitude of the cross bispectrum, known as the squared cross bicoherence, is given by

$$b^2(\omega_j, \omega_k) = \frac{|XB(\omega_j, \omega_k)|^2}{P_1(\omega_j)P_1(\omega_k)P_2(\omega_j + \omega_k)}. \tag{4}$$

It is well known that the squared bicoherence represents the fraction of power at the sum frequency $(\omega_j + \omega_k)$ of the triad owing to quadratic interactions between the two other Fourier modes (ω_j and ω_k) (Kim & Powers, 1979). The quadratic nature of the correlation between in-line and cross-flow motions on a vibrating cylinder have been studied using the cross bispectrum by Vandiver & Jong (1987). Note the definition of cross bispectra allows the use of negative as well as positive frequencies. For a digital time series with Nyquist frequency ω_N, the cross bicoherence is completely described by values within a region consisting of a triangle with vertices at $(\omega_1 = 0,\ \omega_2 = 0)$, $(\omega_1 = \omega_{N/2},\ \omega_2 = \omega_{N/2})$ and $(\omega_1 = \omega_N,\ \omega_2 = 0)$, and an additional triangle with vertices at $(\omega_1 = 0,\ \omega_2 = 0)$, $(\omega_1 = \omega_N,\ \omega_2 = 0)$ and $(\omega_1 = \omega_N,\ \omega_2 = -\omega_N)$. See Lii & Helland (1981) and Choi *et al.* (1985) for detailed discussions of the symmetry properties of cross bispectra.

The data sets considered here were sampled at 30,000 Hz for 1·7 to 17 seconds (Table 1). Each time series (wake velocity and cylinder displacement) was subdivided into segments of 1024 data points, which were fast Fourier transformed to yield the complex Fourier coefficients, $A(\omega_n)$ with a frequency resolution of 29·3 Hz. Tests with different length data segments and windows indicated that a rectangular window 1024 points wide did not result in significant spectral or bispectral leakage or smearing for the data considered here. Cross bispectra were calculated for each 1024-point segment, and then ensemble averaged over the collection of segments. Thus, the bicoherences presented here have 100 to 1000 degrees of freedom. A bicoherence value of $b > 0{\cdot}1$ is statistically significant at about the 95% level for 500 degrees of freedom (Haubrich, 1965).

4. RESULTS

The velocity field in the wake of a vibrating cylinder in low Reynolds number flow has been loosely categorized as either ordered (characterized by a power spectrum

dominated by a narrow primary spectral peak located at the vortex shedding frequency, and associated side band peaks, as well as harmonics of the primary spectral peak, and low frequency peaks), or chaotic (characterized by a relatively broad band wake velocity power spectrum) (Van Atta & Gharib 1987). During many of the experimental runs reported here, once a particular shedding regime was established, the flow field remained essentially unchanged for many minutes, often until the experiment was ended. However, on other occasions, the wake velocity field changed over time, alternating between narrow and broad power spectra. In the following sections the coupling between the vibrating cylinder and the velocity field in its wake is examined for different shedding regimes.

4.1. Ordered Vortex Shedding

Figure 1 displays the power spectrum of wake velocities for the case of ordered vortex shedding (data set number 1 in Table 1). The power spectrum is dominated by a narrow peak at the vortex shedding frequency (referred to as the Strouhal frequency) $f = 850$ Hz (where $f = \omega/2\pi$), with side-band peaks located at $f = 762$ and $f = 938$ Hz, ± 88 Hz from the main peak. Note (Table 1) that 938 Hz is the third harmonic of the fundamental cylinder vibration frequency. There are also peaks (and associated side bands) at $f = 1700$ Hz, the first harmonic of the primary spectral peak, and at $f = 2550$ Hz, the second harmonic. Although some of the frequencies discussed here may not be precise harmonics or exact combinations of other frequencies, they are all identifiable as such within the limits imposed by the frequency resolution of the data. The wake velocity power spectrum also contains two low-frequency peaks, located at $f = 88$ and $f = 176$ Hz (Figure 1).

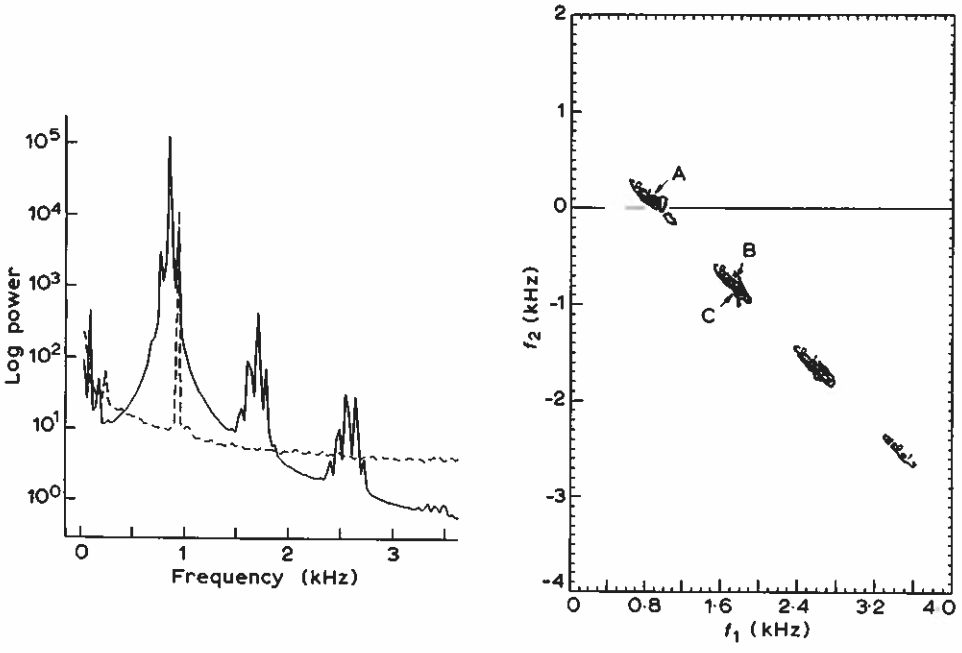

Figure 1. Power spectra (left hand panel) of wake velocity (solid line) and cylinder lateral displacement (dashed line) and contours of cross bicoherence (right hand panel) between wake velocity (f_1 and f_2) and cylinder lateral displacement ($f_1 + f_2$) for ordered vortex shedding (data set number 1, Table 1). The units of power are arbitrary and the minimum value of bicoherence plotted is $b = 0{\cdot}10$, with contours every 0·1.

The power spectrum of the vibrating cylinder (Figure 1) has peaks at $f = 234$ Hz (the lowest natural frequency of the cylinder, as determined by tapping the wind tunnel wall), and at the third harmonic of the cylinder, $f = 938$ Hz. The cylinder is excited by the shedding of vortices at the Strouhal frequency ($f = 850$ Hz), and responds at the harmonic of the lowest mode of oscillation of the cylinder that is closest to the Strouhal frequency.

The coupling between the vibrating cylinder and its wake in ordered shedding is elucidated via the cross bicoherence between wake velocity and cylinder vibration [equation (4)], with the wake velocity measurements providing two Fourier coefficients (the A_1) and the lateral cylinder displacements providing the third coefficient (A_2), as shown in Figure 1. The bicoherence values displayed above the horizontal line through $f_2 = 0$ in Figure 1 represent triads whose two lower frequencies are from the wake velocity field while their sum frequency is from the vibrating cylinder. Below the horizontal line $f_2 = 0$, the vibrating cylinder provides the mode which is located at the frequency representing the difference between the two wake velocity frequencies. Thus, above $f_2 = 0$ the three modes given by the wake $f_1 = 850$, wake $f_2 = 88$, cylinder $f_3 = 938$ Hz are phase coupled, as indicated by the area of high bicoherence values ($b = 0{\cdot}99$) centered at $f_1 = 850$, $f_2 = 88$ Hz in Figure 1 (labeled "A"). This triad consists of the wake-velocity primary spectral peak (850 Hz), the cylinder-displacement primary peak (938 hz), and their difference frequency in the wake velocity field (88 Hz). There is similar coupling (but with lower bicoherence, $b = 0.85$) within the triad consisting of the wake lower side band ($f_1 = 762$ Hz), the cylinder primary peak ($f_3 = 938$ Hz), and their difference frequency in the wake ($f_2 = 176$ Hz).

In Figure 1, below the $f_2 = 0$ line, there are three major areas of significant bicoherence, all of which lie along the same diagonal line. These bicoherence values indicate coupling between triads whose three frequencies include modes representing harmonics and/or side bands from the wake velocity field (f_1 and f_2) such that their sum frequency (recall $f_2 < 0$) $f_3 = 938$ Hz, the frequency of the vibrating cylinder spectral peak. For example, the triads $f_1 = 1700$, $f_2 = -762$, $f_3 = 938$ Hz ($b = 0{\cdot}94$) and $f_1 = 1788$, $f_2 = -850$, $f_3 = 938$ Hz ($b = 0{\cdot}93$) are labeled B and C, respectively, on Figure 1.

4.2. Chaotic Vortex Shedding

Chaotic vortex shedding has been characterized by a broad wake velocity power spectrum, with substantial low frequency energy (Van Atta & Gharib, 1987). An example is shown in Figure 2 (data set 2, Table 1). In this experimental run the Strouhal shedding frequency occurred at $f = 2400$ Hz, 32 times the natural frequency of the cylinder. The cylinder displacement power spectrum also contains peaks at $f = 75$ Hz and $f = 4800$ Hz (Figure 2). Cross bicoherences between the wake velocity and cylinder displacement for the chaotic shedding case (Figure 2) are very similar to those for ordered shedding (Figure 1), indicating coupling between the vibrating cylinder and its wake. The contours along the diagonals "1" through "3" in Figure 2 indicate coupling between wake notions and cylinder vibrations such that the sum frequency of the triads corresponds to cylinder oscillations at approximately $f = 75$, 2400, and 4800 Hz, respectively. For example $b(2454, -2371) = 0{\cdot}35$, $b(2316, 97) = 0{\cdot}97$, and $b(2427, 2371) = 0{\cdot}61$ (the units of frequency are Hz).

4.3. Evolving Shedding Regimes

Some experimental conditions resulted in wake velocity fields with spectra that changed over relatively short periods of time, as shown in Figure 3. The wake was

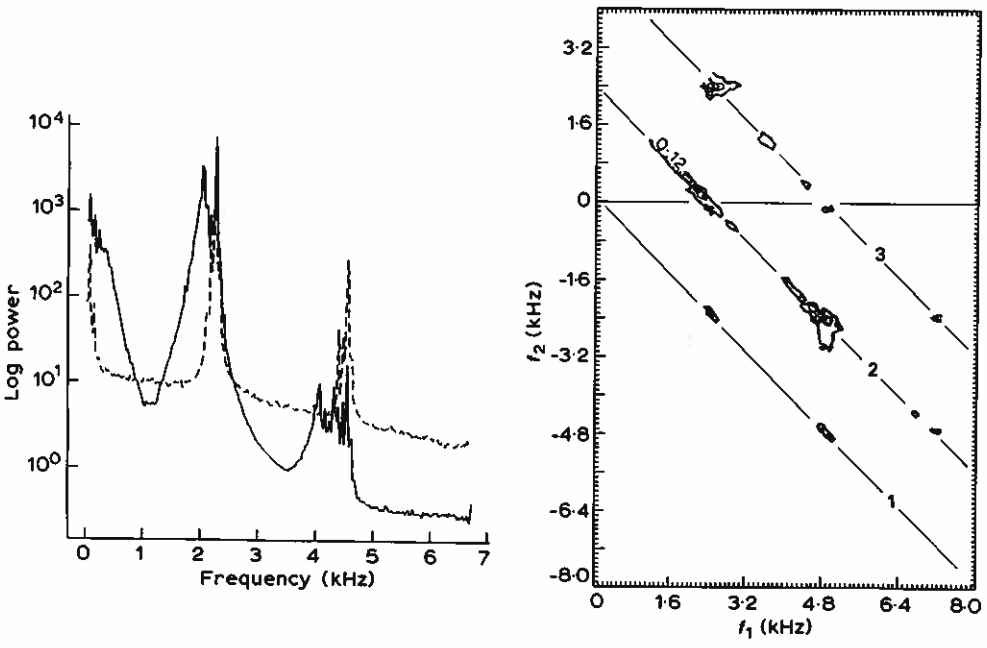

Figure 2. Power spectra (left hand panel) of wake velocity (solid line) and cylinder lateral displacement (dashed line) and contours of cross bicoherence (right hand panel) between wake velocity and cylinder lateral displacement for chaotic vortex shedding (data set number 2, Table 1). The units of power are arbitrary, and the minimum value of bicoherence plotted is $b = 0{\cdot}10$ with contours every 0·1. Note the scale of the frequency axes differ by a factor of 2 from the scale of Figures 1, 3, 4, and 5.

initially dominated by a primary peak [$f = 1640$ Hz, Figure 3(a)] and a sharp upper side band ($f = 1816$ Hz). The power spectrum then developed several sharp peaks at frequencies below the primary peak frequency [Figure 3(b) and (c)], as well as additional low frequency peaks. These peaks blended into each other [Figure 3(d)], and merged with the primary peak ($f = 1640$ Hz), creating a rather broad peak between $f = 1000$ and $f = 1650$ Hz [Figure 3(e) and (f)]. The velocity field spectral peak ($f = 1816$ Hz) that was originally an upper side band of the primary peak became the dominant mode [Figure 3(f) and (g)]. This evolution of the wake velocity power spectrum reversed itself [Figure 3(h–j)], sharp peaks rose at frequencies below the primary peak frequency [Figure 3(i)], and the original primary peak ($f = 1640$ Hz) became the strongest mode once again [Figure 3(j)].

During the experimental run shown in Figure 3, the vibrating cylinder was dominated by two modes of oscillation, approximately 6 and 7 times the fundamental mode, respectively. The higher frequency mode ($f = 1816$ Hz) was observed throughout the experiment, while the lower frequency mode ($f = 1553$ Hz) was transient, as shown in Figure 3. At the beginning of the experiment the vibrating cylinder power spectrum was dominated by the peak at $f = 1816$ Hz [Figure 3(a)]. After about 14 seconds the second peak at $f = 1553$ Hz began to rise [Figure 3(c)], and eventually became the largest peak in the cylinder power spectrum [Figure 3(e)]. Almost immediately, however, the $f = 1553$ Hz peak began to decrease [Figure 3(f)], and 6·8 s after it first appeared [Figure 3(c)], the $f = 1553$ Hz peak was gone [Figure 3(g)]. The $f = 1553$ Hz peak rose again [Figures 3(h, i)], and eventually became equal in level to the $f = 1816$ Hz peak, where it remained for the duration of the experiment [Figure 3(j)].

A third, high-frequency peak in the cylinder spectrum located at $f = 3604$ Hz rose

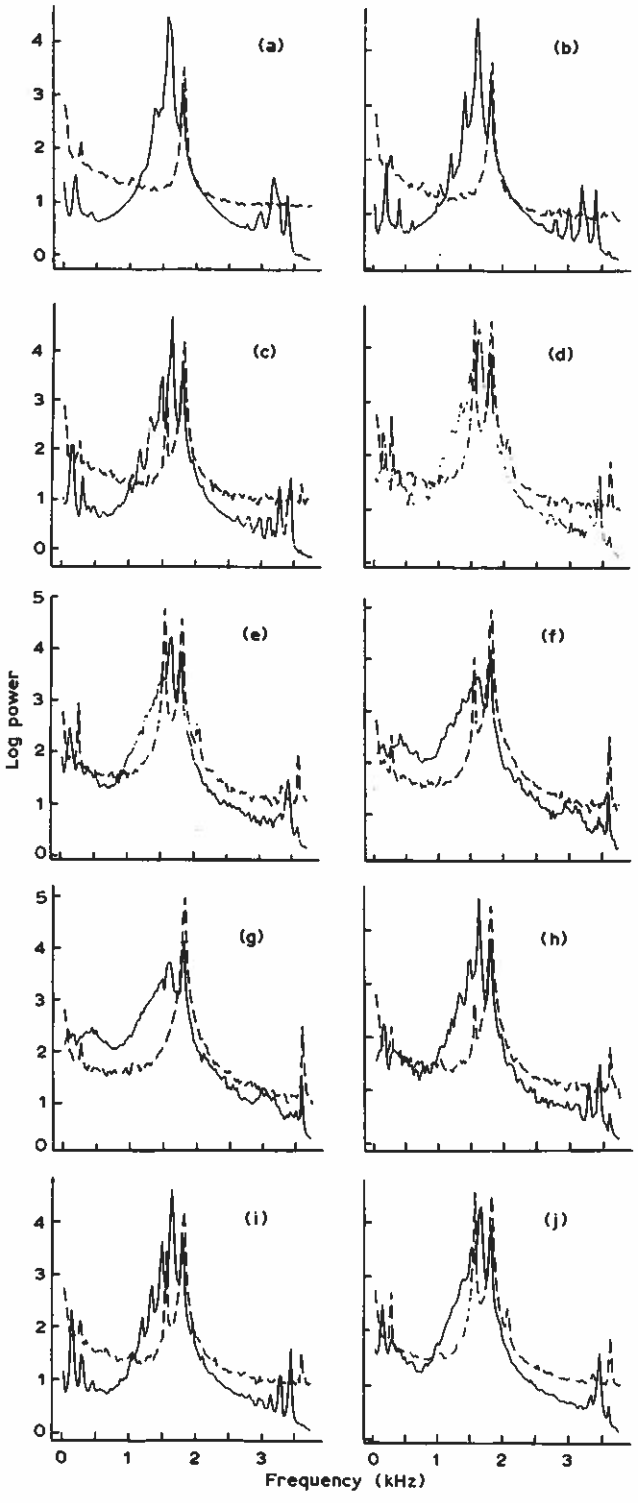

Figure 3. Sequence of power spectra of wake velocity (solid line) and cylinder displacement (dashed line) observed during a 34·1 second experimental run. Individual panels show observations during the following intervals (in seconds): (a) 1–11·9, (b) 11·9–13·7, (c) 13·7–15·4, (d) 15·4–17·1, (e) 17·1–18·8, (f) 18·8–20·5, (g) 20·5–22·2, (h) 22·2–23·9, (i) 23·9–25·6, and (j) 25·6–34·1. The units of power are arbitrary.

out of the background more or less simultaneous with the rise of the $f = 1553$ Hz peak (Figure 3(c, d)], and remained above the background level. On the other hand, the vibrating cylinder peak located at $f = 2050$ Hz was visible only during the times that the two primary peaks $f = 1553$ and $f = 1816$ Hz were approximately equal [Figure 3(d, e, j)]. In separate experimental runs, Van Atta & Gharib (1987) also noticed the vibrating cylinder was alternatively dominated by different modes, many of which were clearly audible.

The reasons why particular cylinder modes dominate are not known (it could be an artifact of the experimental setup), and are not of particular importance here. However, the effect of the various cylinder vibration regimes on the flow field are of interest. For example, Figure 4 (data set number 3 in Table 1) provides an enlarged view of the spectra of Figure 3(j). As briefly mentioned above, the vibrating cylinder power spectrum has two, almost equal primary peaks located at $f = 1553$ and $f = 1816$ Hz, a peak at the lowest natural mode ($f = 263$ Hz), and several higher frequency peaks ($f = 2050$, 3340 and 3604 Hz) at locations corresponding to harmonics of the lowest mode peak (Figure 4). The corresponding wake velocity power spectrum (Figure 4) has a primary peak ($f = 1640$–1670 Hz) located between the two primary cylinder peaks, its side bands ($f = 1523$ and $f = 1816$ Hz), a low-frequency peak ($f = 146$ Hz), and three high-frequency peaks: (i) $f = 3340$ Hz, the first harmonic of the velocity primary ($f = 1670$ Hz); (ii) $f = 3456$ Hz, the sum of the upper side band peak at $f = 1816$ Hz and the velocity primary at $f = 1640$ Hz; (iii) $f = 3604$ Hz, approximately the first harmonic of the velocity spectral peak located at $f = 1916$ Hz.

Noticeably absent from the wake velocity power spectrum in Figure 4 are peaks at $f = 1553$ Hz (corresponding to the cylinder peak at $f = 1553$ Hz), and at frequencies corresponding to possible interactions which involve $f = 1553$ Hz. For example, there are no distinctive peaks in the velocity spectrum (Figure 4) at $f = 117$ Hz (1670–1553), $f = 3193$ Hz (1640 + 1553), $f = 3223$ Hz (1670 + 1553), and so on. It is possible that the oscillation at 1553 Hz in the cylinder has a node close to the location of the hot-wire anemometer. Thus, although the cylinder vibrations at this frequency are detected by the photo detector (located far from the hot wire), the vibrations may be too small along the section of the cylinder located near the hot wire to excite measurable fluctuations in the flow field.

The multitude of couplings between the vibrating cylinder and its wake in the third data set (Figure 4) are displayed in the cross bicoherences shown in Figure 4. Most of the significant bicoherence values fall along the six diagonal lines labeled *1* through *6* (Figure 4). These diagonals (from number 1 to number 6) pass through triads whose sum frequencies (in the cylinder power spectrum) are $f_3 = 263$, 1553, 1816, 2050, 3340, and 3604 Hz, respectively, which correspond to the six peaks in the cylinder power spectrum (Figure 4). Thus, even though there are many peaks in both the velocity and cylinder spectra (Figure 4), the cross-bicoherence spectrum (Figure 4) isolates the phase coupled triads, and clearly demonstrates that every mode of vibration of the cylinder is interacting with the wake. Cross bicoherences for the transient stages shown in Figure 3(b–i) are similar to Figure 4. For example, Figure 5 displays the cross bicoherences for the data of Figure 3(g) (data set 4, Table 1). In this case, there are two dominant modes of cylinder displacement ($f = 1816$ Hz and $f = 3604$ Hz), both of which are phase coupled to the wake velocity field. Thus, the cross bicoherences presented here indicate that the flow field in the wake is responding to changes in the dominant modes of vibration of the cylinder, and the various wake spectra are a direct consequence of cylinder vibrations and subsequent cylinder-wake interactions.

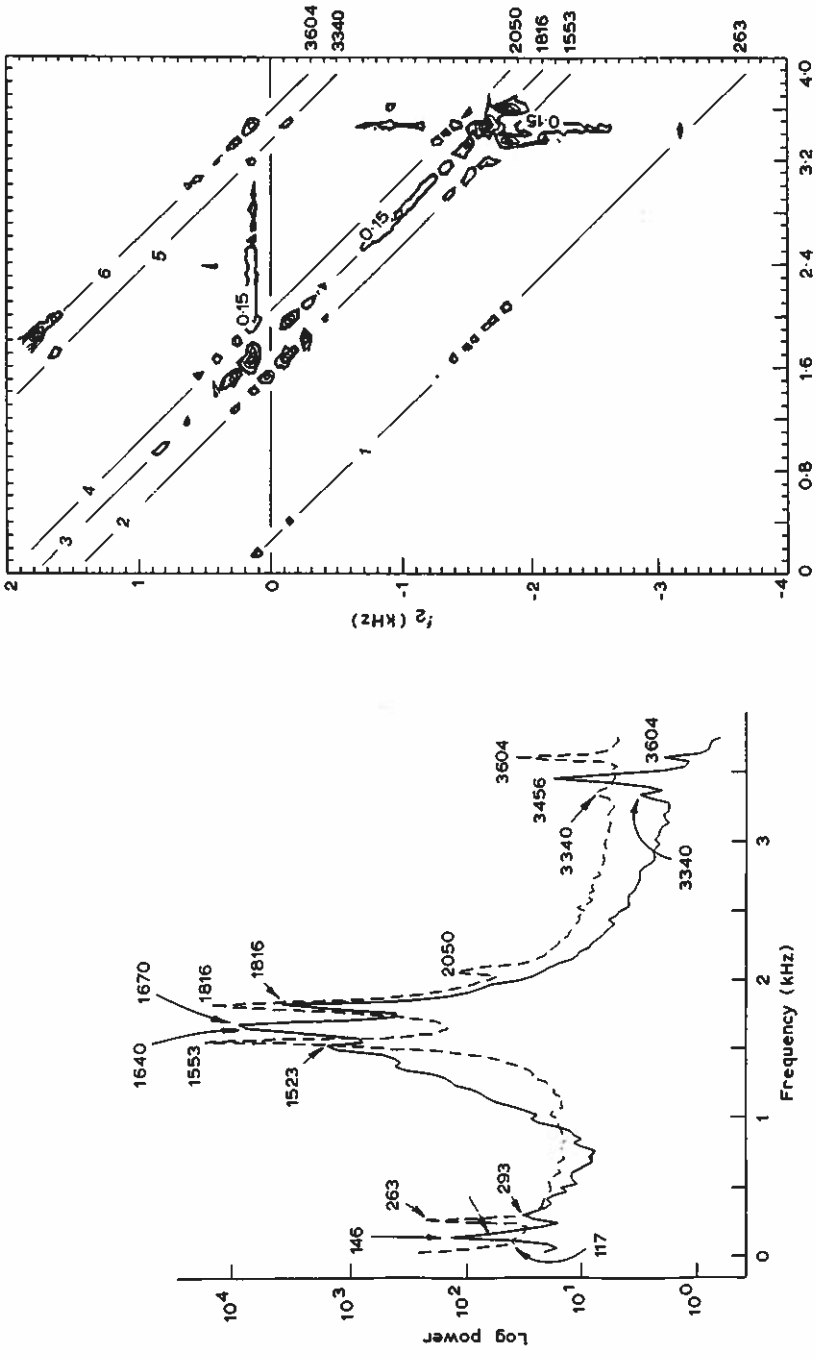

Figure 4. Power spectra (left hand panel) of wake velocity (solid line) and cylinder lateral displacement (dashed line) and contours of cross bicoherence (right hand panel) between wake velocity and cylinder lateral displacement for data set number 3 (Table 1). The units of power are arbitrary, and the minimum value of bicoherence plotted is $b = 0{\cdot}15$, with contours every 0·1.

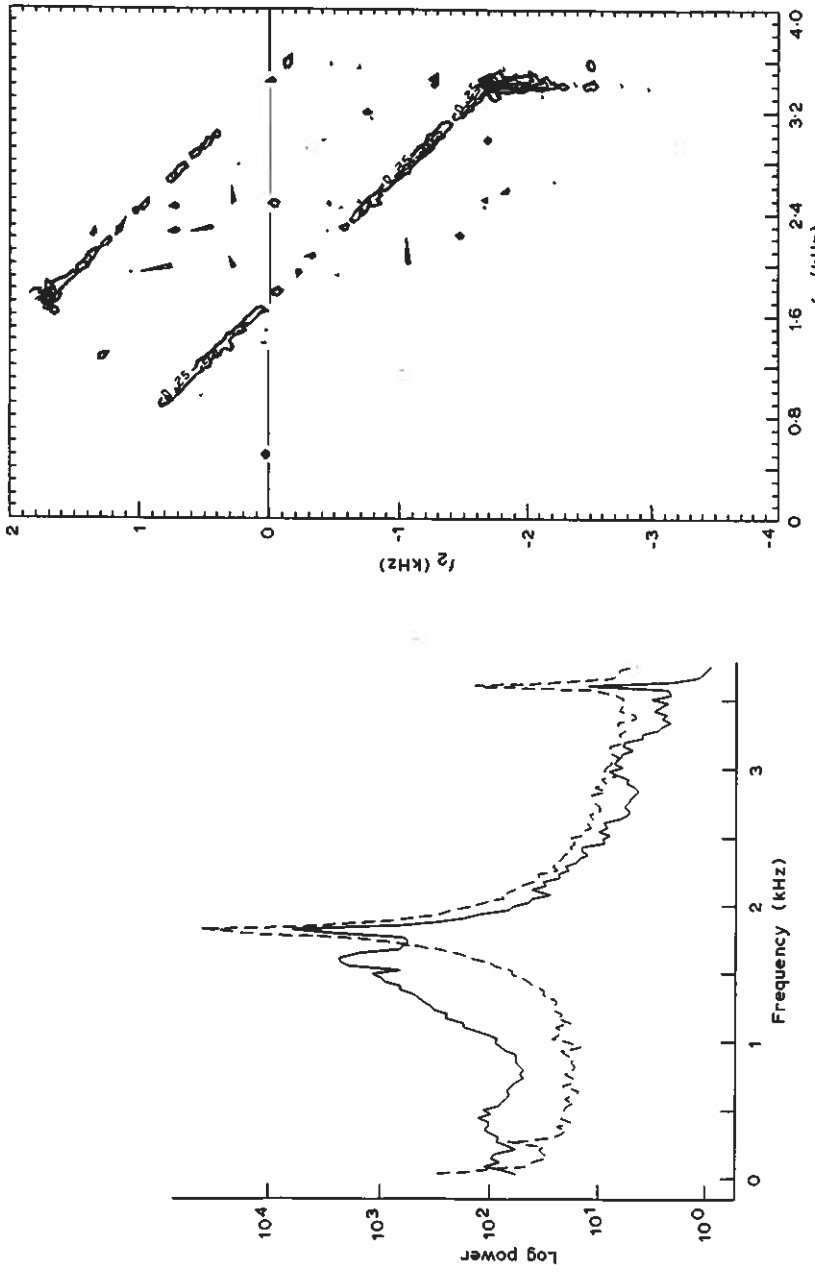

Figure 5. Power spectra (left hand panel) of wake velocity (solid line) and cylinder lateral displacement (dashed line) and contours of cross bicoherence (right hand panel) between wake velocity and cylinder lateral displacement for data set number 4 (Table 1). The units of power are arbitrary, and the minimum value of bicoherence plotted is $b = 0{\cdot}25$ with contours every 0·1.

5. CONCLUSIONS

Velocity spectra in the wake of a slender flexible cylinder in low Reynolds number flows can have a complicated structure. Spectral peaks occur at very low frequencies and at upper and lower side bands of the power spectral primary peak frequency (the Strouhal, or vortex-shedding, frequency) and its harmonics. Simultaneous measurements of wake velocity and cylinder lateral displacement show that vortex shedding excites the cylinder at a natural mode of vibration close to the Strouhal frequency. Cross-bispectral analysis displays the coupling between the vibrating cylinder and its wake, and in particular, isolates the phase coupling between motions measured in the wake and oscillations at their sum and difference frequencies in the vibrating cylinder. Quadratic interactions within the wake between the fluctuations introduced by the cylinder vibrations and fluctuations at the Strouhal frequency lead to low frequency fluctuations as well as motions at side bands of the primary peak and its harmonics.

ACKNOWLEDGMENTS

Support was provided by the Office of Naval Research [Grant N00014-86-K-0877 (S.E.)], the National Science Foundation (Grant OCE 85-11290) and the Defense Advanced Research Projects Agency, University Research Initiative Program (C.V.A. and M.G.). Computations were performed at the San Diego Supercomputer Center (supported by the National Science Foundation). We thank the two anonymous referees who provided detailed and helpful reviews of an earlier version of this paper.

REFERENCES

BEARMAN, P. W. 1984 Vortex shedding from oscillating bluff bodies. *Annual Review of Fluid Mechanics* **16,** 195–222.

BERGER, E. 1967 Suppression of vortex shedding and turbulence behind oscillating cylinders. *Physics of Fluids* **10,** S191–S193.

BERGER, E. & WILLE, R. 1972 Periodic flow phenomena. *Annual Review of Fluid Mechanics* **4,** 313–340.

BLOOR, M. S. 1964 The transition to turbulence in the wake of a circular cylinder. *Journal of Fluid Mechanics* **19,** 290–304.

CHOI, D. W., MIKSAD, R. W., POWERS, E. J. & FISCHER, F. J. 1985 Application of digital cross-bispectral analysis techniques to model the nonlinear response of a moored vessel system in random seas. *Journal of Sound and Vibration* **99,** 309–326.

GERRARD, J. H. 1966 The three-dimensional structure of the wake of a circular cylinder. *Journal of Fluid Mechanics* **25,** 143–164.

GRIFFIN, O. M. 1978 A universal Strouhal number for the 'locking-on' of vortex shedding to the vibrations of bluff cylinders. *Journal of Fluid Mechanics* **85,** 591–606.

GRIFFIN, O. M. & RAMBERG, S. E. 1974 The vortex-street wakes of vibrating cylinders. *Journal of Fluid Mechanics* **66,** 553–576.

GONGWER, C. A. 1952 A study of vanes singing in water. *Journal of Applied Mechanics* **74,** 432–438.

HAUBRICH, R. A. 1965 Earth noises, 5 to 500 millicycles per second. Part 1. *Journal of Geophysical Research* **70,** 1415–1427.

KIM, Y. C. & POWERS, E. J. 1979 Digital bispectral analysis and its applications to nonlinear wave interactions. *IEEE Plasma Science* **1,** 120–131.

KOOPMAN, G. H. 1967 The vortex wakes of vibrating cylinders at low Reynolds numbers, *Journal of Fluid Mechanics* **28,** 501–512.

LII, K. S. & HELLAND, K. N. 1981 Cross-bispectrum computation and variance estimation. *ACM Transactions on Mathematical Software* **7,** 284–294.

POWELL, A. & SHULMAN, A. 1962 Effects of wire resonance on aeolian tones. *Journal of the Acoustical Society of America* **34,** 1146–1147.

Lord RAYLEIGH 1879 Acoustical observations. *The Philosophical Magazine* Series 5, **7,** 149–162.

ROSHKO, A. 1954 On the development of turbulent wakes from vortex streets. NACA Report 1191.

SREENIVASAN, K. R. 1985 Transition and turbulence in fluid flows and low-dimensional chaos. In *Frontiers of Fluid Mechanics* (eds S. W. Davis and J. L. Lumley, pp. 41–67. New York: Springer-Verlag.

STROUHAL, V. 1878 Über eine besondere Art der Tonerregung. *Annalen der Physik and Chemie* **5,** 217–251.

TOEBES, G. H. 1969 The unsteady flow and wake near an oscillating cylinder, *ASME Journal of Basic Engineering* **91,** 493–505.

VAN ATTA, C. W. & GHARIB, M. 1987 Ordered and chaotic vortex streets behind circular cylinders at low Reynolds numbers. *Journal of Fluid Mechanics* **174,** 113–133.

VANDIVER, J. K. & JONG, J. Y. 1987 The relationship between in-line and cross-flow vortex-induced vibration of cylinders. *Journal of Fluids and Structures* **1,** 381–399.

WEHRMANN, O. H. 1965 Reduction of velocity fluctuations in a Karman vortex street by a vibrating cylinder. *Physics of Fluids* **8,** 760–761.